Optical Binding

Michael M. Burns,[1] Jean-Marc Fournier,[1] and Jene A. Golovchenko[1,2]
[1]*Rowland Institute for Science, Cambridge, Massachusetts 02142*
[2]*Harvard University, Cambridge, Massachusetts 02138*
(Received 5 June 1989)

Significant forces between dielectric objects can be induced by intense optical fields. We discuss the origin of these forces which are very long range and oscillate in sign at the optical wavelength. A consequence is that light waves can serve to bind matter in new organized forms. We experimentally demonstrate the simplest case by observing a series of bound states between two 1.43-μm-diam plastic spheres in water, and discuss the extension to more complex cases.

PACS numbers: 41.10.Fs, 42.20.Ji, 78.90.+t

Ashkin[1-4] and others[5] have shown that gradients of time-averaged optical fields can produce forces on microscopic dielectric objects, and by fashioning proper optical gradients have demonstrated trapping. Here we call attention to the apparently little-known fact that intense optical fields can induce significant forces *between* microscopic aggregates of dielectric matter. These forces can result in new ordered states of matter with attendant possibilities for the manipulation and study of systems ranging from small "optical molecules" to extended condensed-matter systems.

The basic ideas can be illustrated in the idealized system of two interacting oscillators separated by a distance r, each consisting of a light particle of mass m and charge e, harmonically bound with resonant frequency ω_0 to a heavy mass of opposite charge. An external optical field, incident on these oscillators, is plane polarized with wave vector $|\mathbf{k}| = \omega/c$. For simplicity we consider the electric field vector such that $\mathbf{E}\times\mathbf{r}$ is perpendicular to $\mathbf{k}$.

In a first approximation the internal motions of each oscillator respond to the Lorentz forces from the external fields alone, which in turn give rise to scattered fields. These scattered fields can be described as originating from a point dipole of time-dependent moment $\mathbf{p}$ located at the position of the heavy mass of each oscillator. The scattered fields from each oscillator acting on its already excited neighbor gives rise to mutual forces between the oscillators.

There are two types of forces that dominate the interaction between the oscillators. The first arises from the induced dipole moment of one oscillator acted on by the gradient of the scattered electric field from the other oscillator. This force is already of a much longer range than those of the standard van der Waals type, since the induced moment (due to the external field) stays constant as the oscillator separation is increased. Perhaps more interesting, however, is the second, magnetic, force that arises from the interaction between the induced currents in the two oscillators. Here the interaction simply results from a Lorentz-force term involving the cross product of the time derivative of the oscillator's dipole moment with the scattered magnetic-flux density from its neighbor. When the vector separation between the two induced currents is perpendicular to the electric field polarization of the incident field this force dominates all others in the scattered-field radiation zone. Again the induced moment and its time derivative stay constant for increasing separation while the radiation field for the magnetic-flux density falls off only inversely with the separation; hence the range is longer than might at first be expected.

For the perturbation treatment discussed above the time dependence of the forces comes from the product of a dipole moment or its time derivative and an electric field gradient or magnetic-flux density. Since both contain the harmonic time dependence of the incident external field, the induced forces between oscillators will have two Fourier time components, one at twice the frequency of the external fields and one at zero frequency. Although the high-frequency forces can have interesting consequences, it is the static (or time-average) part of the force with which the rest of this discussion will deal because it leads to optical binding.

Notice that the static forces we are considering are similar to those normally associated with the radiation pressure of light falling on a single isolated oscillator. In that case it is the phase shift in the internal oscillator motion ultimately connected to the reradiation of the incident field that gives rise to the static force of radiation pressure. In our case it is the phase shift associated with retardation between the oscillators which gives rise to the static internal forces between the oscillators (at least for the long-range part of the interaction). We should therefore not be surprised that spatially oscillatory forces of either sign should arise, because changing the distance between the oscillators results in all possible phase shifts between the induced moments and scattered fields.

Quantitatively the above effects are calculated by solving the coupled classical Maxwell-Lorentz equations self-consistently for the total fields and dynamical state of each oscillator. One then finds for the interaction en-

ergy, W, between the dipole oscillators

$$W = -\tfrac{1}{2}\alpha E^2[yf(x)+y^2g(x)+O(y^3)], \quad (1)$$

with $y=\alpha k^3$ the expansion parameter, $x=kr$, $\beta=\sin^2\vartheta$, and

$$f(x)=[(\beta x^2+2-3\beta)\cos x+(2-3\beta)x\sin x]/x^3,$$

$$g(x)=[4(1-\beta)(\cos x+x\sin x)^2 + \beta(\cos x+x\sin x-x^2\cos x)^2]/x^6.$$

Here ϑ measures the angle between E and the direction connecting the oscillators, and $\alpha=e^2/m(\omega_0^2-\omega^2)$ is the polarizability of the oscillator. When $kr\geq 2\pi$ and $\beta=1$ a satisfactory approximation for the interaction energy is

$$W=-\tfrac{1}{2}\alpha^2E^2k^2\cos(kr)/r. \quad (2)$$

Bound states are obtained at separations near multiple wavelengths, with well depths that fall off inversely with distance between the oscillators.

It is a remarkable fact that even if the oscillators are placed in a conducting fluid (as in our experiments) the static forces responsible for the binding described above are not screened out by free charges. Only plane-wave propagation at high frequencies is needed for the existence of the long-range static influences of interest.

For binding to occur at temperature T we require that $W\gtrsim k_BT$ at the first well ($kr\cong 2\pi$). This constrains the polarizability for which one can achieve significant binding to

$$\alpha > (4\pi k_BT/E^2k^3)^{1/2}. \quad (3)$$

To achieve binding experimentally an intense laser illuminates the oscillators which are realized as small dielectric spheres of radius a and relative index of refraction n for which the polarizability is given by

$$\alpha=a^3(n^2-1)/(n^2+2) \quad (ak<1). \quad (4)$$

The experimental setup is shown in Fig. 1. A 2.2-W argon-ion laser beam (0.387-μm wavelength in water) is focused by two cylindrical lenses of different focal lengths to form a narrow line about 3 μm wide and 50 μm long at the common focal plane in the sample cell. The polarization of the beam is chosen so that E is perpendicular to the long axis of this trap. The sample (polystyrene spheres in water) is viewed either by diffraction of the incident beam on a screen 20 cm from the cell, or via an imaging system that collects the light from the incident beam in a projection-microscope arrangement onto a screen (see Fig. 1).

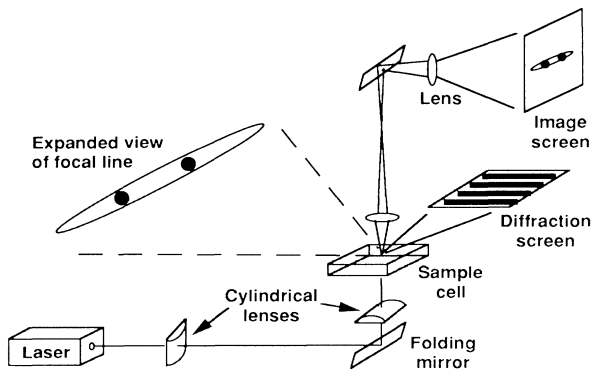

FIG. 1. Experimental setup for optical binding.

The sample cell is made of two fused-silica plates separated by 200 μm. A dilute concentration of monodisperse 1.43-μm-diam polystyrene spheres in water (relative index 1.20) with $10^{-4}M$ phosphite buffer is placed between the plates. The screening by the buffer (Debye length about 300 Å) eliminates all static monopole forces arising from any static charge on the spheres, but (as described above) has no effect on the interactions that we seek to explore here.

By manipulating the cell while observing the projected image it is possible to put two isolated spheres into the trap, initially separated by some distance—say 5 μm —and observe their interaction with time. Because of the strong gradient of the applied field in a direction perpendicular to the focal line, the spheres are constrained to move in one dimension along the line. Radiation pressure along the beam axis presses the two spheres against the upper cell surface, assuring the interaction geometry discussed earlier.

The relative distance separating the two spheres is determined from the fringe spacing on the diffraction screen. A video camera connected to a standard VCR records the time course of the fringes. Frame-by-frame measurement of the fringe pattern yields the separation of the two spheres at $\frac{1}{30}$-sec intervals. A plot of the relative separation of two spheres (measured in units of the wavelength of the light in water) for one 17-sec period is shown in Fig. 2, along with a histogram of the separations.

It is quite evident that as the spheres move together driven by diffusive forces and a weak optical gradient, there are discrete separations at which they are more likely to be found, and that these differ by distances approximately equal to the wavelength of the light, just as the above arguments indicated. The trajectory looks like that of a particle exhibiting fluctuating Brownian motion in a potential with periodic wells. The closest approach at about 3.8 wavelengths (1.43 μm) is in fact the separation for two spheres in contact. Higher laser power would mean deeper traps, and, assuming no additional thermal heating, longer dwell times near each minimum of the potential of Eq. (2). The laser power was chosen so the system hopped between many different wells during the time window of an experimental run.

For a number of technical reasons we have not yet been able to perform our experiments with spheres so small that $ka<1$. The problems include thermal heat-

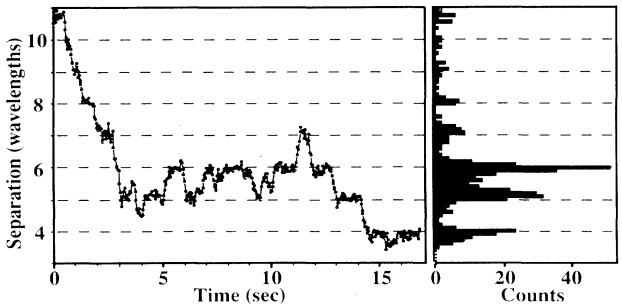

FIG. 2. Relative separation of two 1.43-μm-diam spheres measured in units of wavelength of illuminating light in water. The plot on the left shows the time course of the separation, sampled at $\frac{1}{30}$-sec intervals, and the plot on the right is the corresponding histogram.

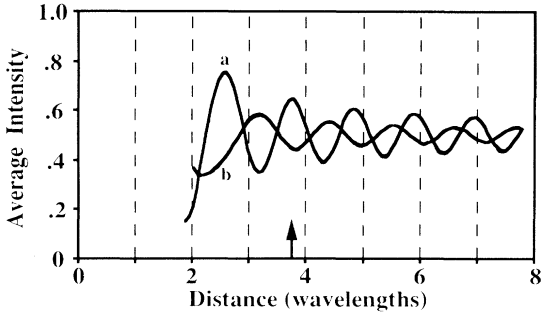

FIG. 3. Mie calculations of the time-average intensity of the near fields of (curve *a*) 1.43- and (curve *b*) 1.53-μm spheres. The arrow indicates the distance separating two identical spheres when touching.

ing of the spheres, poor image and diffraction signal-to-noise ratio, and thermal fluctuation times shorter than the sampling period. Thus while we retain the physical intuition contained in Eqs. (1)–(4), detailed numerical comparisons are inappropriate. An extension of the discrete-dipole approximation of Purcell and Pennypacker[6,7] is currently being implemented for detailed calculations. Here we take an intermediate, simplified approach to discuss our $ka \gtrsim 2\pi$ experimental case. The spheres are assumed to scatter light according to the exact (near-field) Mie equations[8] and the interference of this scattered light with the incident wave forms potential wells corresponding to those in the dipole calculation considered above. This simplified approach is similar to the introductory perturbation viewpoint in that the multiple-scattering fields's contributions are not considered. In actual fact these contributions are probably not negligible, but they affect the magnitude of the forces much more than the spatial location of the maxima and minima.

A plot of the time-average intensity near a single sphere calculated in this manner is shown in Fig. 3, curve *a*. It is expected that the spheres, reacting to the gradient force, will find potential minima at those places where peaks in the light intensity occur. Notice that the intensity peaks do asymptotically approach one-wavelength spacings at the larger distances, just as the dipole calculations predict. Note also that when the spheres are close together the peaks are separated by more than one wavelength, with the first physically accessible peak occurring at about 3.8 wavelengths—just the contact condition, and also the nearest approach noted in the experimental observations.

To appreciate the close correspondence between the data and calculations, curve *b* of Fig. 3 shows a plot of the intensity for a slightly different size sphere—here 1.53 μm. Notice that the intensity peaks occur at very different relative locations because of the changed phase shifts of the scattered partial waves. Notice also that the intensity contrast, and hence potential well depth, is less as well. In fact, the 1.43-μm spheres are an optimum size; at any nearby size the binding potential would be less, and the first potential well would be at a distance other than the contact distance.

In conclusion, we have discussed and demonstrated the basic physics underlying the process of optical binding. This new interaction between bits of dielectric matter may well find application in the purposeful organization of both small and extended microscopic systems. Of course much more complicated structures than the one dealt with here can be envisioned; for example, increased dimensionality and number of spheres should yield a rich array of organized stable structures worthy of study in their own right. These organizations can be compared and contrasted with arrays of particles confined by mechanisms other than the one discussed here.[9,10] We mention that optically induced and organized structures formed in a liquid environment may be maintained in the absence of the applied field by freezing.

Finally we note that many readers of this journal view forces between elementary particles of nature as originating from the exchange of virtual quanta of fields to which they are coupled. The induced interaction discussed in this paper fits nicely into that scheme, but with real quanta being exchanged.[11] We wonder whether other particles and fields may be substituted for our dipoles and light, yielding analogous effects in other domains of physics.

We wish to thank Professor N. Bloembergen and Professor E. Purcell for useful discussions, Hang Xu for calculational assistance, and the Rowland Institute for Science for its continued support.

[1]A. Ashkin, J. M. Dziedzic, J. E. Bjorkholm, and S. Chu, Opt. Lett. **11**, 288 (1986).

[2]A. Ashkin, Phys. Rev. Lett. **24**, 156 (1970).

[3]A. Ashkin, Science **210**, 1081 (1980).
[4]A. Ashkin and J. M. Dziedzic, Science **187**, 1073 (1975).
[5]See references in S. Stenholm, Rev. Mod. Phys. **58**, 699 (1986).
[6]E. M. Purcell and C. R. Pennypacker, Astrophys. J. **186**, 705 (1973).
[7]B. T. Draine, Astrophys. J. **332(2)**, 848 (1988).
[8]H. C. van de Hulst, *Light Scattering by Small Particles* (Dover, New York, 1981).
[9]N. A. Clark, A. J. Hurd, and B. J. Ackerson, Nature (London) **281**, 57 (1979).
[10]C. A. Murray and D. H. Van Winkle, Phys. Rev. Lett. **58**, 1200 (1987).
[11]T. Thirunamachandran, Mol. Phys. **40**, 393 (1980).